Protoplasma (1999) 209: 105–119

PROTOPLASMA

Three-dimensional organization and dynamic changes of the actin cytoskeleton in embryo sacs of *Zea mays* and *Torenia fournieri*

B.-Q. Huang[1], **Y. Fu**[1,2], **S. Y. Zee**[1,*], and **P. K. Hepler**[3]

[1] Department of Botany, The University of Hong Kong, Hong Kong, [2] College of Life Sciences, Wuhan University, Wuhan, and [3] Department of Biology, University of Massachusetts, Amherst, Massachusetts

Received October 28, 1998
Accepted March 11, 1999

Summary. Actin organization was observed in *m*-maleimidobenzoic acid N-hydroxysuccinimide ester(MBS)-treated maize embryo sacs by confocal laser scanning microscopy. The results revealed that dynamic changes of actin occur not only in the degenerating synergid, but also in the egg during fertilization. The actin filaments distribute randomly in the chalazal part of the synergid before fertilization; they later become organized into numerous aggregates in the chalazal end after pollination. The accumulation of actin at this region is intensified after the pollen tube discharges its contents. Concurrently, actin patches have also been found in the cytoplasm of the egg cell and later they accumulate in the cortical region. To compare with MBS-treated maize embryo sacs, we have performed phalloidin microinjection to label the actin cytoskeleton in living embryo sacs of *Torenia fournieri*. The results have extended the previous observations on the three-dimensional organization of the actin arrays in the cells of the female germ unit and confirm the occurrence of the actin coronas in the embryo sac during fertilization. We have found that there is an actin cap occurring near the filiform apparatus after anthesis. In addition, phalloidin microinjection into the Torenia embryo sac has proved the presence of intercellular actin between the cells of the female germ unit and thus confirms the occurrence of the actin coronas in the embryo sac during fertilization. Moreover, actin dynamic changes also take place in the egg and the central cell, accomplished with the interaction between the male and female gametes. The actin filaments initially organize into a distinct actin network in the cortex of the central cell after anthesis; they become fragmented in the micropylar end of the cell after pollination. Similar to maize, actin patches have also been observed in the egg cortex after pollination. This is the first report of actin dynamics in the living embryo sac. The results suggest that the actin cytoskeleton may play an essential role in the reception of the pollen tube, migration of the male gametes, and even gametic fusion.

Keywords: Actin dynamics; Embryo sacs; Fertilization; Microinjection; *Torenia fournieri* Lind.; *Zea mays* L.

* Correspondence and reprints: Department of Botany, University of Hong Kong, Pokfulam Road, Hong Kong.

Abbreviations: DIC differential interference contrast; MBS *m*-maleimidobenzoic acid N-hydroxysuccinimide ester.

Introduction

In flowering plants, fertilization involves a complex sequence of events, in which one sperm fuses with egg and another sperm fertilizes the central cell, leading to the formation of the zygote and endosperm (Jensen 1974, Russell 1992). In most species the prominent features of this process include the following: the degeneration of one of the synergids, its subsequent penetration by the pollen tube, discharge of the pollen tube cytoplasm and male gametes into the synergid, migration of sperm cells to the fusion site between the egg, synergid and central cell, and fusion of each sperm with a female target cell (Russell 1992). These processes are believed to be accomplished through a complex series of events induced by the interaction between the male and female gametes, in which the cytoskeleton appears to play an important role (Russell 1996).

In plant reproduction, a considerable amount of information has been collected concerning the male reproductive system. Cytoskeletal elements have been found to participate in pollen tube elongation, organelle transport, and the descent of generative and sperm cells (Palevitz and Tiezzi 1992, Pierson and Cresti 1992). In contrast to the male reproductive cells, the information concerning the organization and possible involvement of the actin cytoskeleton in female reproductive cells is still scarce (Bednara et al. 1990,

Huang et al. 1993, Huang and Russell 1994, Webb and Gunning 1994).

The involvement of the cytoskeleton during fertilization has only been examined in a few species including *Plumbago zeylanica* (Huang et al. 1993), *Nicotiana tabacum* (Huang and Russell 1994), and *Zea mays* (Huang and Sheridan 1998). Previous studies have revealed that changes of the actin cytoskeleton occur during fertilization. The prominent feature is the formation of two actin coronas: one overarching the chalazal periphery of the degenerating synergid and the other overarching the interface between the egg and central cell, and between the egg and synergids (Huang and Russell 1994, Huang and Sheridan 1998). The presence of these actin coronas, however, raises additional questions. How do these actin coronas form and how do their dynamic changes proceed? Is this dynamic change of actin an independent event occurring only in the degenerating synergid or is the egg cell also involved? How does fertilization trigger the reorganization of actin in the cells of the "female germ unit"? What is the role of the actin cytoskeleton in the reception, migration of male gametes, and fusion between the male and female gametes?

In this study we have used confocal microscopy to examine the three-dimensional organization of the actin cytoskeleton in *m*-maleimidobenzoic acid N-hydroxysuccinimide ester (MBS)-treated maize embryo sacs to address some of the aforementioned questions. We have found that dynamic changes of the actin cytoskeleton occur not only in the synergid, but also in the egg cell and the central cell during fertilization. The dynamic changes of the actin filaments within the cells of the female germ unit may reflect a series of events essential for fertilization. We have also shown the organization and changes of actin filaments in the living embryo sacs of *Torenia fournieri* by microinjection in order to compare the actin dynamics with those of the MBS-treated embryo sacs in maize.

Material and methods

Plant material

Plants of maize were grown as previously described (Huang and Sheridan 1994). When the silks emerged, the ears were hand-pollinated and collected 16 to 18 h after pollination and then processed for embryo sac isolation, *m*-maleimidobenzoic acid N-hydroxysuccinimide ester (MBS) treatment, and rhodamine-phalloidin staining as described below.

Torenia fournieri was grown in the greenhouse under a 14 h photoperiod at 25 °C in the Department of Biology, University of Massachusetts at Amherst. The flowers were collected at two days after opening, and the ovules were then dissected for microinjection.

Isolation of embryo sacs and staining of actin filaments

Aldehyde fixation method

Embryo sacs were processed for actin labeling by aldehyde fixation and then treated with MBS as described previously (Sonobe and Shibaoka 1989, Huang et al. 1993) and modified as below. The ovaries were cut and immediately fixed in the mixture of fixative consisting of 4% paraformaldehyde, 10% dimethylsulfoxide, 400 μM MBS (Sigma, St. Louis, Mo., U.S.A.) in PMEG buffer (50 mM piperazine-N,N′-bis(2-ethanesulfonic acid), pH 6.9, 2 mM $MgSO_4$, 5 mM ethylene glycol-bis(β-aminoethylether)-N,N,N′,N′-tetraacetic acid [EGTA], and 4% glycerol) for 2 h at room temperature. Ovules were then incubated for 45 min at 37 °C in an enzyme solution containing 1% cellulysin (Calbiochem, La Jolla, Calif., U.S.A.), 1% pectinase, and 0.3 % pectolyase mixed in PMEG buffer containing 2 mM phenylmethylsulfonyl fluoride, 25 μM pepstatin, 25 μM leupeptin as protease inhibitors. After rinsing with PMEG buffer, the materials were incubated for 40 min in a solution of 0.33 μM rhodamine-phalloidin (Molecular Probes, Eugene, Oreg., U.S.A.) and 1 μg of Hoechst 33258 per ml. Preparations were subsequently mounted in Slowfade solution (Molecular Probes).

MBS crosslinking method

Ovules were dissected directly into a solution of 0.6 M sorbitol containing 400 μM MBS and protease inhibitors (2 mM phenymethylsulphonyl fluoride, 25 μM pepstatin, 25 μM leupeptin) for 2 h. MBS was prepared with dimethylsulfoxide in a 100× stocking solution. The embryo sacs were partially isolated by direct dissection using a Leitz DM IRB inverted microscope. The isolated embryo sacs were then incubated in a solution of 0.33 μM rhodamine-conjugated phalloidin (Molecular Probes) for 3 h. The preparations were subsequently mounted in a sorbitol solution and observed with a Leica TCS NT confocal microscope. Three-dimensional images of the actin cytoskeleton in the embryo sacs were recorded by the Leica TCS NT confocal-microscopy software.

Microinjection of living embryo sacs in T. fournieri

Preparation of microinjecion

Ovules were dissected and immediately immobilized in a microscope slide chamber in a thin layer of 1% low-temperature-gelling agarose, type VII (Sigma), containing 0.025% Triton X-100, and then cultured in the growth medium as described by Valster and Hepler (1997). An aliquot of 5 μl of Alexa-phalloidin (Molecular Probes) stock solution in methanol (6.6 μM) was used for preparation of the injection solution. Methanol was evaporated under vacuum for 30 min, then the preparation was resuspended in 20 μl injection buffer (100 mM KCl, 2 mM N-2-hydroxyethylpiperazine-N′-2-ethanesulfonic acid at pH 7.0) to make a final concentration of 1.67 μM Alexa-phalloidin solution. The co-injection solution for labeling actin filaments and nuclear DNA was prepared with the injection buffer to a final concentration of 2 μM Alexa-phalloidin and 20 μg of propidium iodide (PI) per ml. The injection solution was centrifuged at 20,000 rpm for 15 min at room temperature and its supernatant was then loaded in the capillaries of the microinjector.

Microinjection and microscopy

Since the embryo sac of *T. fournieri* protrudes from the micropyle of ovules after blooming (Higashiyama et al. 1997), it is easily accessible for microinjection. The microinjection was carried out following the procedure described by Valster and Hepler (1997) and Vos and Hepler (1998). The injection solution was loaded in the capillary glass needle with a 1 mm diameter (World Precision Instruments, Sarasota, Fla., U.S.A.) and mounted in a pressure syringe system (Eppendorf, Brinkmann Instruments, Westbury, N.Y. and Gilmount Instruments, Barrington, Ill., U.S.A.). The cells of the embryo sac were pressure injected with precision micromanipulators (Narishige, Greenvale, N.Y., U.S.A.) mounted on the inverted Nikon microscope equipped with a ×40 wide-angle oil immersion lens. The cells were examined with a Bio-Rad MRC-600 confocal scanning microscope or a Leica TCS NT confocal scanning microscope. Both DIC and fluorescent images of the embryo sacs were collected by the MRC-600 COMOS software or the Leica TCS NT software. Images were further processed by Adobe Photoshop 4.0 (Adobe, San Jose, Calif., U.S.A.).

Results

Organization and dynamic changes of the actin cytoskeleton in the maize embryo sac before and during fertilization

A typical mature embryo sac of maize consists of an egg apparatus, a central cell, and a variable number of antipodal cells (Huang and Sheridan 1994). Figures 1a and 2a show the partially isolated maize embryo sacs, in which the central cell and antipodal cells could be clearly observed. The distribution of actin filaments in the egg cell is illustrated in Fig. 1b and c. A dense array of actin filaments is found at the chalazal end of the egg cell at the median plane of the embryo sac (Fig. 1b, c). Abundant actin filaments emanate from the nucleus of the central cell and extend to the transvacuolar strands (Fig. 2b), where they are organized into a network (Fig. 2c). In the cortex of the central cell, actin filaments are transversely oriented, which are perpendicular to the long axis of the embryo sac (Fig. 2d). Actin filaments in the antipodal cells display a reticulate arrangement in the cytoplasm. These cells also contain a number of vacuoles (Fig. 3a, b).

Syngamy is most prevalent from 16–19 h after pollination in maize (Huang and Sheridan 1998). Before the tip of the pollen tube arrives at the receptive synergid, notable changes of the actin cytoskeleton occur in the central cell. Actin filaments become organized into a meshwork in the cytoplasm of the central cell, while transversely aligned actin filaments appear somewhat sparser in the micropylar cortex (Fig. 4a, b). Several vacuoles fill the cavity of the central cell, thus restricting the distribution of the actin filaments to cytoplasmic strands and to the cortical region. This is particularly conspicuous at the cytoplasm-rich chalazal region (Fig. 5a–c). Some of the actin filaments become organized into a complex network in the cortical region (Fig. 5b, c).

Figure 6a shows the actin labeling in the egg cell of a partially isolated embryo sac at the median plane. Since a large vacuole occupies most of the micropylar end of the egg cell, the actin cytoskeleton is mainly restricted to the chalazal cytoplasm. Changes in the actin filaments also occur in the egg cell during fertilization, including (1) a prominent band located in the cortex (Fig. 6a), and (2) discrete actin patches distributed in the cytoplasm. The latter appear to be more concentrated near the micropylar end (Fig. 6b, c).

A partially isolated unfertilized embryo sac, where the synergid and the egg could be identified in the micropylar end, is shown in Fig. 7a. In the synergid, actin filaments are found to be randomly aligned in the chalazal part (Fig. 7b). This pattern of actin distribution could be seen either before pollination or after pollination. However, dramatic changes of the actin cytoskeleton take place when the synergid degenerates. During fertilization the actin cytoskeleton in the degenerating synergid appears to produce numerous punctate aggregates, which are distributed throughout the cell. The aggregates accumulate at the chalazal end of the degenerated synergid and at the interface between synergid and egg cell, and between egg cell and central cell, forming two distinct actin coronas (Fig. 8a, b), which could be also visualized by staining with rhodamine-phalloidin in aldehyde-fixed embryo sacs (Fig. 9a). During fertilization, the sperm cells appear to pass along these corona bands and eventually fuse with the egg and central cell (Fig. 9b) (also see Huang and Sheridan 1998). The corona bands in the embryo sac disappear before the division of the zygote (Huang and Sheridan 1998).

Three-dimensional organization and dynamic changes of the actin cytoskeleton in living female germ unit of T. fournieri

The localization of the actin cytoskeleton has also been examined by microinjection of Alexa-phalloidin into living embryo sacs. Due to the inaccessibility of maize embryo sacs and technical difficulties in performing the microinjection, we have conducted these experiments with the naked embryo sacs of *T. fournieri*. The cells of the female germ unit are

accessible because the embryo sacs protrude from the micropyle after anthesis.

Like other typical embryo sacs, the female germ unit in *T. fournieri* consists of an egg apparatus and a central cell. The two synergids occupy the micropylar end of the embryo sac and contain a distinct filiform apparatus, which is attached to the basal wall of the synergids and extends from the common wall between two synergids (Higashiyama et al. 1997). The synergid is polarized and characterized by a large vacuole

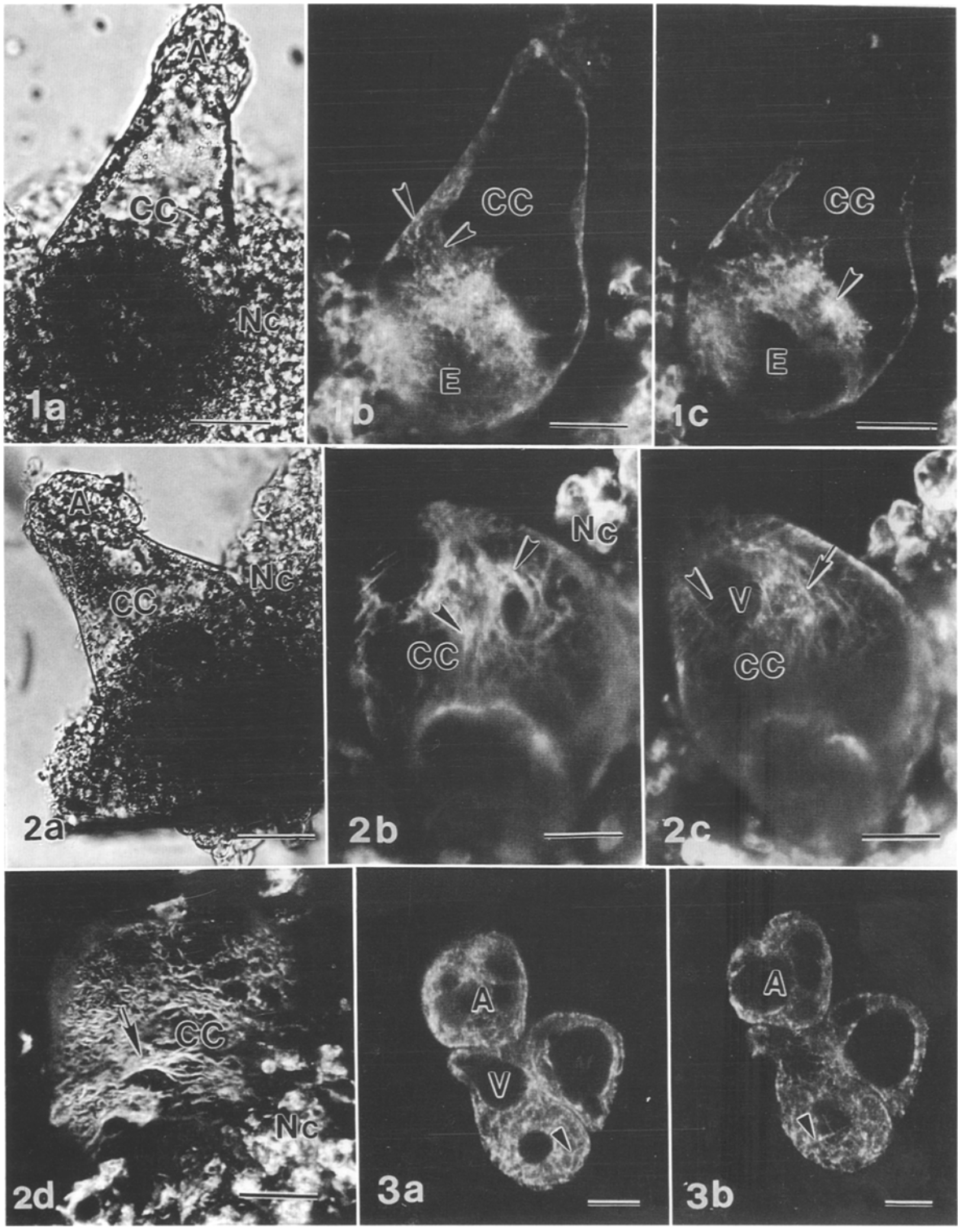

located at the chalazal end (Fig. 10a). Due to the specific location of synergids and the thick cell wall at the filiform apparatus, microinjection of the synergid appears to be a technical challenge. This barrier has been overcome by microinjecting the synergids through the micropyle of the embryo sac and the middle lamella of the synergid common wall. Microinjection of Alexa-phalloidin into the synergid cell of the embryo sac before pollination has revealed sparse actin filaments distributed at the chalazal end (Fig. 10b), where they are aligned randomly at the cortex (Fig. 10c). In the micropylar cytoplasm of the cell, however, some of the actin filaments become organized into thick bundles (Fig. 10d).

The egg cell is spherical in shape (Fig. 11a) and its nucleus is located in the center of the cell (Higashiyama et al. 1997). The egg is located adjacent to the synergid and characterized by the presence of cytoplasmic strands emanating from the nucleus (Higashiyama et al. 1997). In comparison to the synergid and central cell, the egg cell appears to be mostly inaccessible. Therefore, the microinjection of the egg cell has to be carried out either by penetrating via the middle lamella between the two halves of the filiform apparatus or at the micropylar lateral region of the embryo sac. Due to this technical difficulty, the rate of success is low (3–5%). However, microinjection of Alexa-phalloidin has revealed the existence of a network of actin filaments in the egg cell that is distributed throughout the cytoplasm (Fig. 11b).

Most of the central cell is visible as it protrudes from the ovular tissue at two days after flower opening. Before fertilization the secondary nucleus is located in the chalazal or central region of the central cell, where cytoplasmic strands are seen to emanate from it (Fig. 12). Since the central cell is easily accessible, the rate of success for microinjection was up to 60%. Microinjection of Alexa-phalloidin into the central cell of the embryo sac before pollination revealed a prominent network of actin in the cortical region (Fig. 13 a–c) and some sparse, transversely aligned actin filaments at the micropylar end (Fig. 13a, c). Actin filaments could also be seen in the cytoplasmic strands at the median plane (Fig. 13d).

Two days after anthesis, at the stage in which the flower has a freshly opened stigma, two synergids and an egg cell are evident at the micropylar end of the embryo sac (one of the synergids is not in the focal plane) (Fig. 14a). Phalloidin microinjection of the synergid has revealed an actin cap near the region of the filiform apparatus at the micropylar end of the synergids, where the distribution of actin is dense (Fig. 14 b). It disappears after the pollen tube penetrates the degenerated synergid (unpubl. obs.). At about 5 h after pollination, but before pollen tube arrival, one of the synergids has begun to degenerate. The egg cell is distinct with a nucleus in the center. The egg cell occupies most of the micropylar end of the embryo sac (Fig. 15a). Microinjection of Alexa-phalloidin into the degenerated synergid reveals that there is a distinct

Figs. 1–3. Localization of actin cytoskeleton in the maize embryo sac before fertilization

Fig. 1a–c. Three-dimensional organization of the actin cytoskeleton in a partially isolated embryo sac before fertilization, visualized by staining with rhodamine-phalloidin in MBS-treated embryo sac. **a** A partially isolated embryo sac with the micropylar end towards the bottom of the field. Note that most part of the embryo sac was exposed after microdissection. *CC* Central cell, *A* antipodal cell, *Nc* nucellus. Phase contrast. **b** A confocal image of the same embryo sac as shown in **a**. Note that transverse actin filaments (arrowheads) are aligned in the cortical region of the central cell (*CC*) and a dense array of actin filaments in the egg cytoplasm (*E*). **c** A median confocal section of the same embryo sac as in **a**, showing a dense actin array (arrowhead) at the chalazal periphery of the egg cell (*E*) and a large vacuole in the micropylar region of the cell. Bars: 50 μm

Fig. 2a–d. Three-dimensional organization of the actin cytoskeleton in the central cell before fertilization visualized by staining with rhodamine-phalloidin in MBS-treated embryo sac. **a** A partially isolated embryo sac. Note that half of the chalazal part of the embryo sac (at the top end of the picture) is exposed after being microdissected. Phase contrast. *A* Antipodal cell, *CC* central cell, *Nc* nucellus. **b** A median confocal optical section of the same embryo sac as in **a**. Actin bundles are evident throughout the cytoplasmic strands and particularly dense in the perinuclear region (arrowheads) of the central cell (*CC*). **c** An optical section of the same embryo sac as in **a**, showing transversely aligned actin filaments in the cortex (arrowhead) and dense actin bundles in the transvacuolar cytoplasmic strands (arrow) in the central cell (*CC*). *V* Vacuole. **d** An optical section at the periphery of the same embryo sac as in **b**, showing transversely aligned actin filaments in the cortex of the central cell (arrow). Bars: 50 μm

Fig. 3a, b. The organization of actin filaments in the antipodal cells. **a** A confocal optical image of the antipodal cells in one of the isolated embryo sacs. Note that reticulate actin filaments (arrowhead) are distributed in the cytoplasm. A number of vacuoles (*V*) are present throughout the cells. **b** A different optical section of antipodal cells (*A*) as shown in **a**. An actin network is evident in the cytoplasm (arrowhead) in this section. Bars: 10 μm

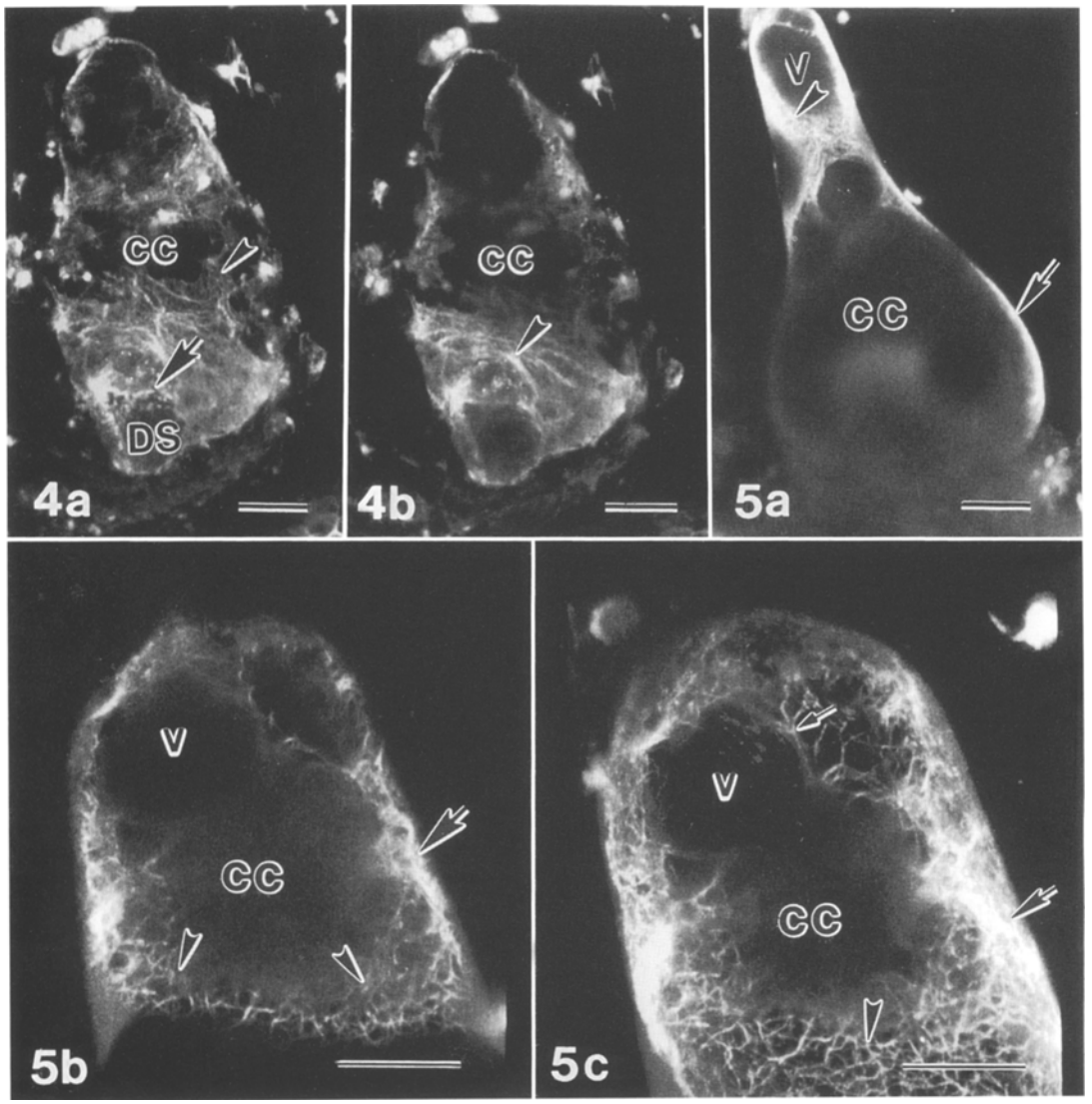

Figs. 4 and **5.** *Localization of the actin cytoskeleton in the fertilized maize embryo sac*

Fig. 4a, b. Organization of the actin cytoskeleton in the embryo sac during fertilization. **a** An embryo sac during fertilization. Note that the actin aggregates (arrow) are accumulated at the chalazal end of the degenerated synergid (*DS*). An anastomosing network (arrowhead) is evident in the cytoplasm of the central cell (*CC*). **b** A different optical section of the same embryo sac in **a**, showing transversely aligned actin filaments (arrowhead) in the cortex of the central cell (*CC*) in the micropylar end. Bars: 50 μm

Fig. 5a–c. Three-dimensional organization of actin filaments in the central cell during fertilization. **a** A fertilized embryo sac stained with rhodamine-phalloidin showing an actin meshwork in the chalazal cytoplasm (arrowhead) of the central cell (*CC*) and a dense actin array in the cortex (arrow). *V* Vacuole. Bar: 50 μm. **b** The same embryo sac as in **a** reveals a meshwork of actin filaments (arrowheads) in the cytoplasm of the central cell (*CC*). Note the delimiting circumferential actin bundles near the cortex (arrow). Bar: 20 μm. **c** A different optical section of the same central cell as in **b**. Note that actin bundles are aligned in the transvacuolar strand (small arrow) and a prominent network is distributed throughout the cytoplasm (arrowhead). Dense actin bundles are evident in the cortex of the cell (large arrow). Bar: 20 μm

actin band at the interface of the degenerated synergid and egg cell. Actin is profusely distributed in the degenerated synergid. Some actin appear to aggregate into a dense mass (Fig. 15b). After the pollen tube has penetrated and discharged its contents into the degenerated synergid (Fig. 16a, pollen tube is not in the focal plane), abundant actin aggregates accumulate at the interface between the degenerated synergid and the persistent synergid (Fig. 16b). These observations are consistent with the previous findings in *Nicotiana tabacum* (Huang and Russell 1994) and maize (Huang and Sheridan 1998: figs. 8a, b and 9a), indicating that

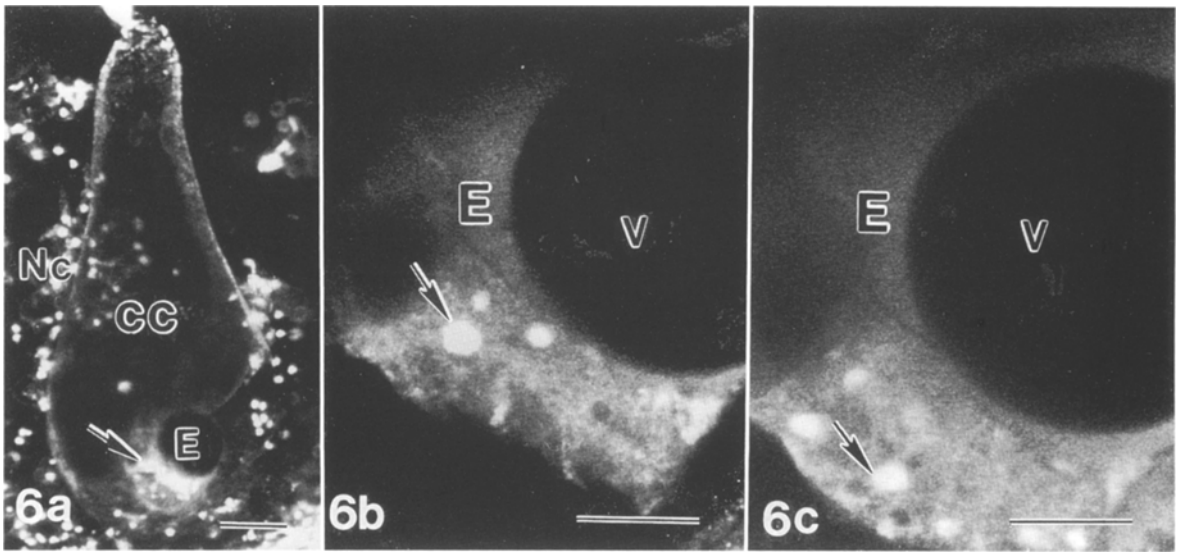

Fig. 6a–c. Dynamic changes of actin cytoskeleton in the egg cell during fertilization. **a** Staining with rhodamine-phalloidin in a fertilized embryo sac reveals a prominent actin band (arrow) at the periphery of the egg cell (*E*). *Nc* Nucellus. Bar: 50 μm. **b** An optical image of actin cytoskeleton in the same egg cell as in **a**. Note that actin patches (arrow) are distributed in the chalazal cytoplasm of the egg cell (*E*). *V* Vacuole. Bar: 20 μm. **c** A serial confocal image of the same cell shown in **b** indicates that the actin patches (arrow) are accumulated at the periphery of the cell. *V* Vacuole. Bar: 20 μm

changes in the actin cytoskeleton accompany the interaction between the male and female gametes. At about 5 h after pollination, before the arrival of the pollen tube, intercellular actin can also be observed by microinjection of Alexa-phalloidin into the intercellular space between the egg and central cell. It emerges as a distinct corona (Fig. 17 a, b). Sometimes two actin bands could be observed (dependent on the site of penetration of the microinjection needle) in the intercellular space between the cells of the female germ unit. One band appears in the intercellular space between synergid and egg and the other between egg and central cell (Fig. 17 c). Similar to maize, the actin cytoskeleton in the Torenia egg also displays remarkable changes after pollination. Microinjection of Alexa-phalloidin into the egg cell after pollination reveals that there are numerous actin patches in the cortex of the egg cell (Fig. 18). The dynamic change of the actin cytoskeleton also occurs in the central cell after pollination. Microinjection of the central cell at two days after flowering reveals that the central cell displays a prominent actin network at the cortex, which is particularly dense in the perinuclear region of the secondary nucleus and also at the micropylar end (Fig. 19 a). However, at 5 h after pollination the dynamic changes of actin in the central cell become more evident. The actin network becomes fragmented in the micropylar end of the central cell (Fig. 19 b). When nuclear fusion occurs between a sperm nucleus and the secondary nucleus, the actin network completely depolymerizes into punctate structures. This involves a series of very complex events which will be reported in another communication.

Discussion

Methods for labeling of actin cytoskeleton in the embryo sacs: a comparison

Due to inaccessibility of the embryo sac and technical difficulties involved with actin preservation in the female reproductive cells, attempts to localize actin filaments in the aldehyde-fixed cells with rhodamine-phalloidin have only been partially successful in a few species (Bednara et al. 1990, Huang et al. 1993, Huang and Russell 1994, Webb and Gunning 1994, Ye et al. 1997). Since the embryo sac has a large volume and is highly vacuolated, it requires a rapid and adequate fixation. This is particularly true for the fertilized embryo sac, which processes rapid and dynamic events. Aldehyde fixation has been found to induce significant morphological changes in cell integrity during fertilization due to inadequate chemical fixation (Russell 1982). The collapse of synergid and egg cell sometimes has been observed in the fertilized embryo sac of maize when fixed with paraformalde-

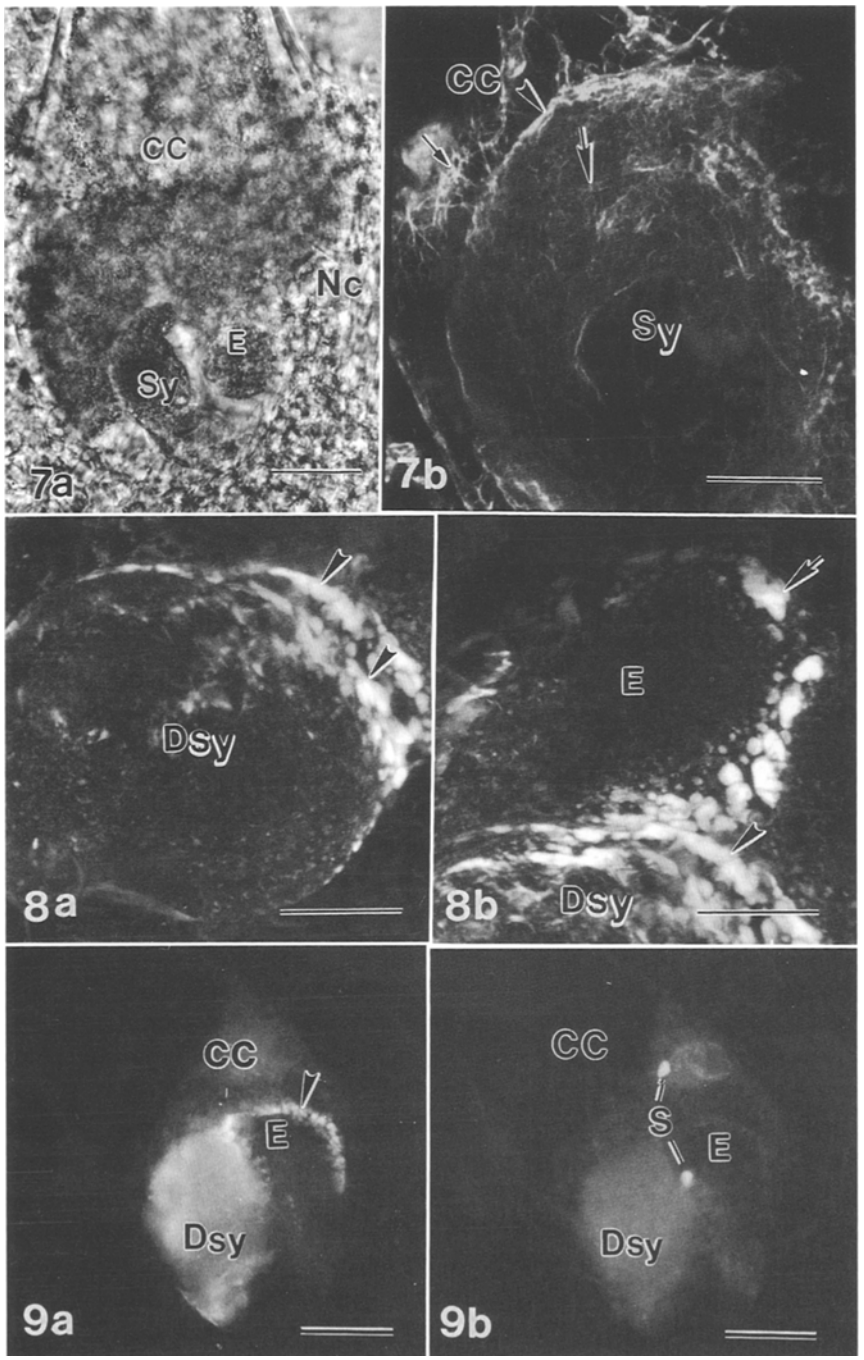

Figs. 7–9. Dynamic changes of actin cytoskeleton in the synergid during fertilization in maize

Figs. 7a, b. Organization of actin cytoskeleton in the synergid after pollination. **a** A partially isolated embryo sac. Phase contrast image. *Sy* synergid, *E* egg cell, *CC* central cell, *Nc* Nucellus. **b** Staining of rhodamine-phalloidin of the same embryo sac as in **a**, showing actin distribution in the synergid before degeneration. Note that the actin filaments (large arrow) are randomly distributed at the chalazal part of the synergid (*Sy*) and a dense array of actin filaments is aligned along the chalazal cortex (arrowhead). A meshwork of actin filaments (small arrows) is present in the central cell (*CC*). Bars: 20 μm

Fig. 8a, b. Dynamic changes of actin cytoskeleton in the degenerating synergid during fertilization. **a** A fertilized embryo sac stained with rhodamine-phalloidin showing abundant dots and aggregates of actin distributed throughout the degenerated synergid (*Dsy*). They accumulate at the chalazal end of the degenerated synergid, forming a distinct corona band (arrowheads). **b** Two actin coronas are present in the egg apparatus of the same embryo sac as in **a**. One corona overarches at the interface between egg cell (*E*) and central cell (arrow) and another in the chalazal end of the degenerated synergid (*Dsy*) (arrowhead). Bars: 20 μm

Fig. 9a, b. Syngamy in the embryo sac. **a** Staining of rhodamine-phalloidin in a formaldehyde-fixed embryo sac showing actin coronas (arrowhead) in the egg apparatus. *CC* Central cell; *Dsy* degenerated synergid; *E* egg cell. **b** Staining with Hoechst 33258 in the same embryo sac showing that one sperm cell (*S*) approaches the egg cell (*E*), and the second sperm cell fuses with the central cell (*CC*). *Dsy* Degenerated synergid. Bars: 50 μm

hyde (unpubl. obs.). Thus, paraformaldehyde fixation gave images with sparse actin filaments due to the poor preservation of actin cytoskeleton (Fig. 9a). Of concern, the process of cell wall digestion with enzymes and membrane permeabilization with dimethylsulfoxide and EGTA may result in deleterious effects on the actin filaments (Heslop-Harrison and Heslop-Harrison 1991, Doris and Steer 1996).

To circumvent aforementioned problems in labeling actin cytoskeleton due to the conventional aldehyde fixation method, we have introduced the MBS cross-linking method to avoid using enzymes, EGTA, and any detergent and to minimize deleterious effects on the actin cytoskeleton. The partially isolated maize embryo sacs were only treated with the mild protein-cross-linking reagent MBS to stabilize filamentous (F)

actin (Sonobe and Shibaoka 1989). With the aid of confocal microscopy, we were able to clearly visualize three-dimensional organization and dynamic changes of the actin cytoskeleton in the maize embryo sac. These changes not only occur in the synergid but also in the egg cell during fertilization, and include the formation of actin coronas in the egg apparatus and actin patches in the egg cortex. Here we have shown further by using the technique of microinjection of Alexa-phalloidin that changes in the dynamics of the actin cytoskeleton observed in maize embryo sacs also occur in the living embryo sacs of *T. fournieri*. This indicates that localization of the actin cytoskeleton in the maize embryo sac by the MBS cross-linking method is not an artifact of the treatment; however, adequate time must be given during MBS treatment if the cells are to be properly stabilized and fixed (Doris and Steer 1996).

Phalloidin microinjection is an approach that may avoid some of the aforementioned concerns in the labeling of actin cytoskeleton in plant cells (Lloyd 1989, Cleary 1995, Valster and Hepler 1997). In addition, it permits one to observe living cells in "action". Application of this technique for studying the actin cytoskeleton in the embryo sac, however, is difficult due to the inaccessibility of the female gametophyte. *Torenia fournieri*, the plant material chosen for microinjection is ideal for studying the events during fertilization in living embryo sacs, because it has a naked embryo sac that protrudes from the micropyle (Higashiyama et al. 1997). Thus, all the cells of the female germ unit are clearly visible under the light microscope. Attempts in artificial fertilization by microinjecting sperm cells into the egg apparatus also have been carried out using this plant material (Keijzer et al. 1988, Keijzer 1992).

In this study we have shown for the first time that three-dimensional arrays of F-actin can be clearly visualized in living embryo sacs. Furthermore, most of the observations in the living embryo sacs confirm the findings reported previously, e.g., in *Nicotiana tabacum*, maize, and *Plumbago zeylanica* (Huang and Russell 1994, Huang and Sheridan 1998, Huang et al. 1993). But some of the features have not been observed in fixed and even MBS-treated embryo sacs. For instance we have identified longitudinally oriented actin bundles present in the micropylar cytoplasm of the synergid in addition to the randomly oriented arrays in the chalazal part of the cell. Moreover, in comparison with MBS-treated embryo sacs of maize before pollination, in *T. fournieri* transversely aligned actin filaments in the cortex of the central cell are much sparser and tend to concentrate mainly in the micropylar end of the central cell. Furthermore, the actin filaments in the cortex of the central cell after anthesis invariably organize into a distinct network. They become fragmented in the micropylar end of the central cell after pollination. But in maize, only a meshwork of actin filaments is present in the cytoplasm of the central cell after pollination. Whether actin fragmentation also occurs in maize after pollination remains to be answered by further investigation. Microinjection also allows us to examine the precise location and dynamic changes of the actin cytoskeleton in the female germ unit. After microinjection of Alexa-phalloidin into the synergid, we are able to expose the actin dynamics in the synergid during fertilization. One novel finding in the microinjected embryo sac is the existence of an actin cap near the filiform apparatus. These actin filaments emerge from the filiform apparatus when the embryo sac becomes mature and the stigma is competent to accept pollens; they disappear after the pollen tube penetrates the embryo sac (unpubl. obs.).

Microinjection of Alexa-phalloidin into the living Torenia embryo sac also reveals that actin coronas do occur during fertilization. Phalloidin microinjected into the synergid also shows that the actin corona at the chalazal end does emerge before the pollen tube arrives at, and penetrates, the embryo sac (see Fig. 15 b). The fluorescence of the coronas is intensified at the chalazal end of the degenerated synergid and intercellular space between the egg, synergids and central cell after the pollen tube discharges its contents. As in *Nicotiana tabacum* and maize, two actin coronas could be localized in the Torenia embryo sac during fertilization if Alexa-phalloidin is precisely microinjected into the intercellular space between the egg and central cell and between the synergids and central cell. However, more frequently only one corona can be localized and this we attribute to the fact that often only the degenerating synergid could be easily microinjected and this type of microinjection usually will only label one corona (Fig. 15 a, b) instead of two. Thus the data obtained with *T. fournieri* confirm the previous observations of the occurrence of actin coronas in the fertilized embryo sacs in *Plumbago zeylanica* (Huang et al. 1993), *Nicotiana tabacum* (Huang and Russell 1994), and maize (Huang and Sheridan 1998; also the present study). Furthermore, phalloidin microinjection also localizes the actin

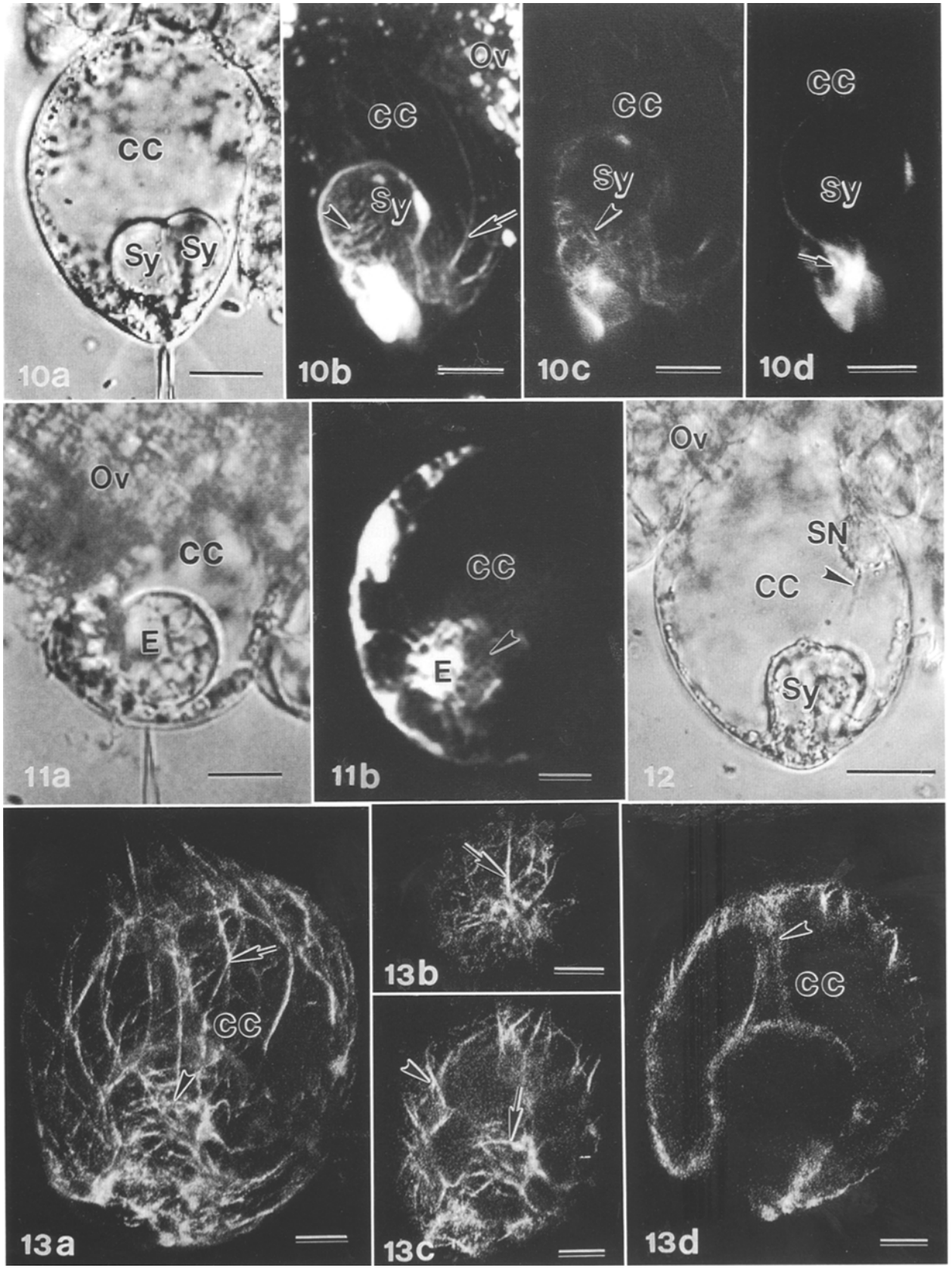
CC
Sy
Sy
10a
Ov
CC
Sy
10b
CC
Sy
10c
CC
Sy
10d
Ov
CC
E
11a
CC
E
11b
Ov
SN
CC
Sy
12
CC
13a
13b
13c
CC
13d

aggregates to the intercellular space between egg and central cell and between the synergids and the central cell during fertilization confirming the existence of actin in the intercellular space between the cells of the female germ unit reported previously using fixed embryo sacs (Huang and Russell 1994).

The role of actin cytoskeleton during fertilization

Our results, along with previous findings, indicate that the reorganization of the actin cytoskeleton in the embryo sac occurs simultaneously with a series of fertilization events including reception of the pollen tube, migration of male gametes, and gametic fusion. The reception of the pollen tube and male gametes in the synergid is the first step to secure gametic fusion. Depolymerization or fragmentation of the cytoskeleton appears to be a crucial event accompanied by the degeneration of one of the synergids before pollen tube arrival. Supporting this view is the localization of actin aggregates in the cytoplasm and an actin corona at the chalazal end of the degenerating synergid (Huang and Russell 1994). The localization of the actin corona at the chalazal end of the degenerating synergid before pollen tube arrival is also illustrated in *T. fournieri* in this study. This suggests that the actin corona may initially derive from the actin cytoskeleton of the synergid; the release of pollen tube contents is not a necessary prerequisite for corona formation (Huang and Russell 1994, Huang and Sheridan 1998). The actin filaments in the degenerating synergid appear to depolymerize into dots and then accumulate as aggregates at the chalazal end of the cell. These aggregates may infiltrate into the intercellular gap after the breakdown of the plasma membrane of the synergid, possibly creating a pathway taken by the sperm cells in fusing with the egg and the central cell.

Structural studies have demonstrated that synergids contain an extremely high concentration of calcium (Chaubal and Reger 1990, 1992). In fertilized ovules, abundant membrane-bound calcium has also been detected in the degenerated synergid (Huang and Russell 1992). Presumably, the release of calcium from the vacuoles in the degenerating synergid alters the local physiological conditions, causing fragmentation and depolymerization of both actin microfilaments and microtubules. These events may be a necessary prelude to the reception of the pollen tube and the male gametes.

Transport and deposition of the sperm cells to the fusion sites of the female target cells is a second step for gametic fusion. Since plant sperm cells are immobile, the pollen tube and embryo sac must provide a means for their transport to the female target cells. The location of the actin coronas along the path of the gametes has led to the hypothesis that they may play a role in sperm migration (Huang and Russell 1994). Supporting this hypothesis is the observation that myosin I has been detected on the surface of the generative and sperm cells (Miller et al. 1995); its interaction with the adjacent actin microfilaments could provide the necessary motive force.

Figs. 10–13. Actin distribution in the living embryo sacs of *T. fournieri* before pollination

Fig. 10a–d. Labeling of actin filaments in the synergid by microinjection with Alexa-phalloidin and then recorded by serial optical sections. **a** A mature embryo sac of *T. fournieri* before fertilization. Note that the embryo sac protrudes from the ovular tissue. Two synergids (*Sy*) and a large central cell (*CC*) are evident in the protruding embryo sac. The egg cell is not in the focal plane. DIC. **b** Microinjection of Alexa-phalloidin in the same embryo sac shown in **a**. Sparse actin filaments (arrowhead) in the chalazal end and dense labeling in the micropylar end in one of the synergids (*Sy*) are evident. Some actin filaments (arrow) in the central cell (*CC*) are also labeled. *Ov* Ovular tissue. **c** An optical section of the same synergid as in **b**, showing the presence of random actin filaments in the cortex (arrowhead). **d** Labeling of actin in the same synergid (*Sy*) as in **b** reveals actin bundles (arrow) aligned at the micropylar end of the cell in another optical section. Bars: 50 μm

Fig. 11a, b. Labeling of actin filaments in the egg cell with microinjection of Alexa-phalloidin. **a** A mature embryo sac protrudes from the ovular tissue (*Ov*). The egg cell (*E*) is evident in the micropylar end of the embryo sac. *CC* Central cell. DIC. Bar: 50 μm. **b** Microinjection of Alexa-phalloidin into the egg cell (*E*) revealing an actin meshwork (arrowhead) in the cytoplasm of the egg cell. Bar: 20 μm

Fig. 12. DIC image of a living embryo sac showing a large central cell (*CC*) and two synergids (*Sy*). Note that the secondary nucleus (*SN*) is visible at the central region where the cytoplasmic strands (arrowhead) emanate from it. *Ov* Ovular tissue. Bar: 50 μm

Fig. 13a–d. Actin distribution in a microinjected central cell (*CC*). **a** The projection of serial optical sections showing an actin network (arrow) and some transversely aligned actin filaments in the cortex of the central cell (arrowhead). **b** An optical section in the cortex showing an actin network in the same central cell as in **a**. **c** An image of the same central cell as in **a** at different focal plane showing some sparse transversely aligned filaments (arrow) at the micropylar end and a network of actin filaments (arrowhead) in the cortex. **d** A median optical section of the same central cell (*CC*) showing some actin filaments in the cytoplasmic strands (arrowhead). Bars: 20 μm

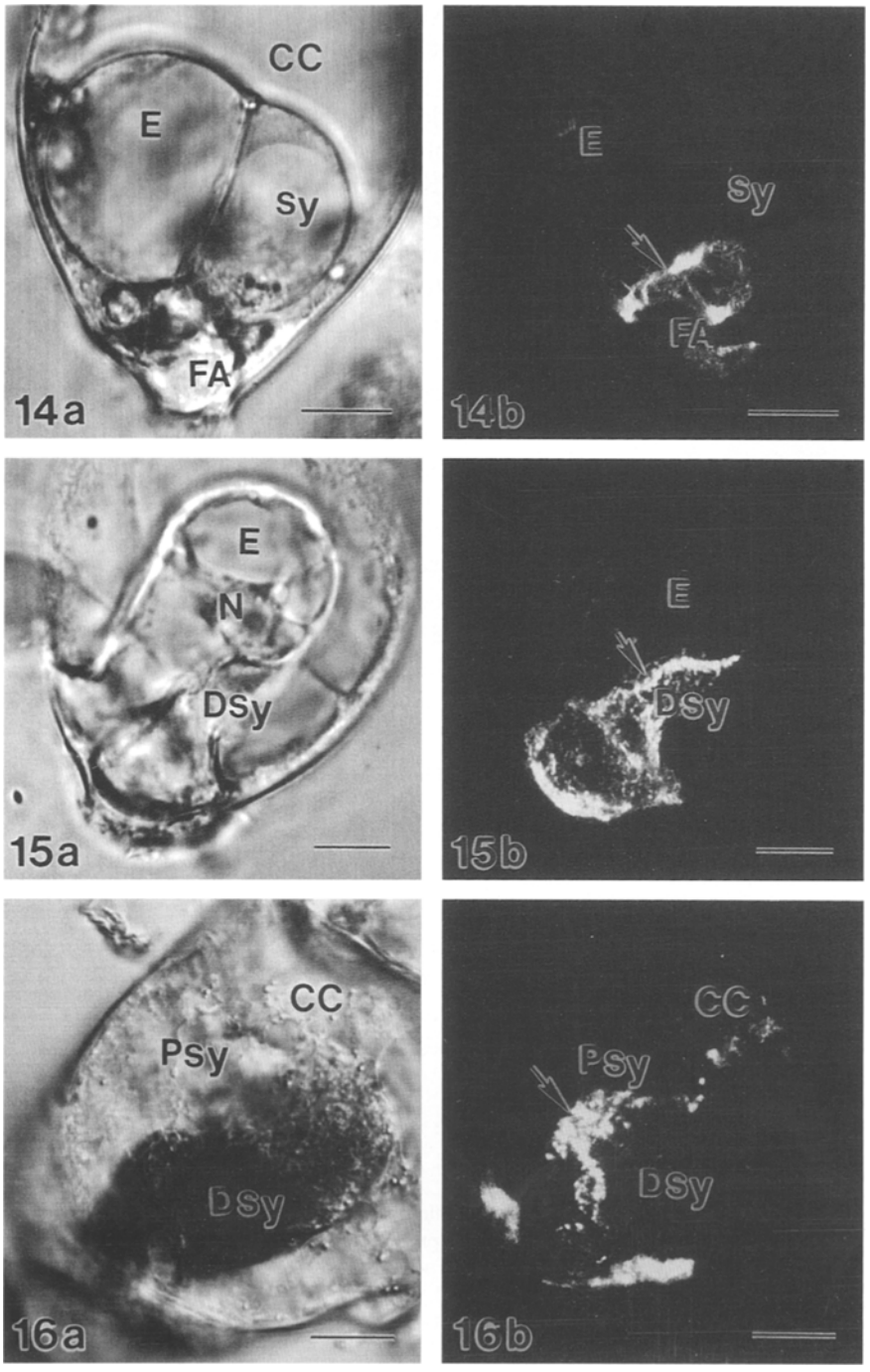

Figs. 14–16. Actin dynamics in the synergid of *T. fournieri* during fertilization

Fig. 14a, b. Actin organization in the filiform apparatus of the synergids before pollination. **a** DIC image of the embryo sac showing a synergid (*Sy*) and an egg cell (*E*) at the micropylar end of the embryo sac (the other synergid is not in the same focal plane). Note that a large vacuole is still evident in the chalazal end of the synergid. *CC* Central cell; *FA* filiform apparatus. **b** Phalloidin microinjection of the same synergid (*Sy*) as in **a** reveals that there is an actin cap associated with the filiform apparatus (*FA*). Note that at places the distribution of actin is dense (arrow). Bars: 10 μm

Fig. 15a, b. Labeling of actin in a degenerated synergid at 5 h after pollination but before the arrival of pollen tube. **a** A transmissional image of the embryo sac showing an egg (*E*) and a degenerated synergid (*Dsy*) at the micropylar end (the other synergid is not in focal plane). Note that the egg nucleus (*N*) locates in the center of the cell. **b** Microinjection with Alexa-phalloidin into the degenerated synergid (*Dsy*) reveals that actin is profusely distributed throughout the degenerated synergid. Some actin appears to have aggregated into dense mass. A distinct actin band at the chalazal end of the degenerated synergid adjacent to the egg cell (*E*) (arrow) is also visible. Bars: 10 μm

Fig. 16a, b. Labeling of actin in a degenerated synergid of an embryo sac after pollen tube discharge. **a** Viewed from the micropylar end of the fertilizing embryo sac (*CC*). Note that a degenerated synergid (*Dsy*) is evident at the micropylar end of the embryo sac. *Psy* Persistent synergid. **b** Microinjection with Alexa-phalloidin through the micropylar end of the same embryo sac as in **a** reveals that actin aggregates (arrow) are concentrated at the interface between the degenerated synergid (*Dsy*) and the persistent synergid (*Psy*). Bars: 10 μm

Gametic fusion is an essential event of fertilization in which actin may participate. The information from other systems has demonstrated that gametic fusion is accompanied by reorganization of the actin cytoskeleton (Hart and Fluck 1995, Swope and Kropf 1993). It is accomplished by depolymerization-repolymerization or rearrangement of preexisting actin filaments (Shimizu 1995) including the formation of the fertilization cone (Hart and Fluck 1995) and actin patch (Swope and Kropf 1993) for sperm entry. Similarly, during fertilization a prominent actin band has been found in the cortex of the egg cell and discrete actin patches are localized in the cytoplasm. The reorganization of the actin cytoskeleton in the egg cell

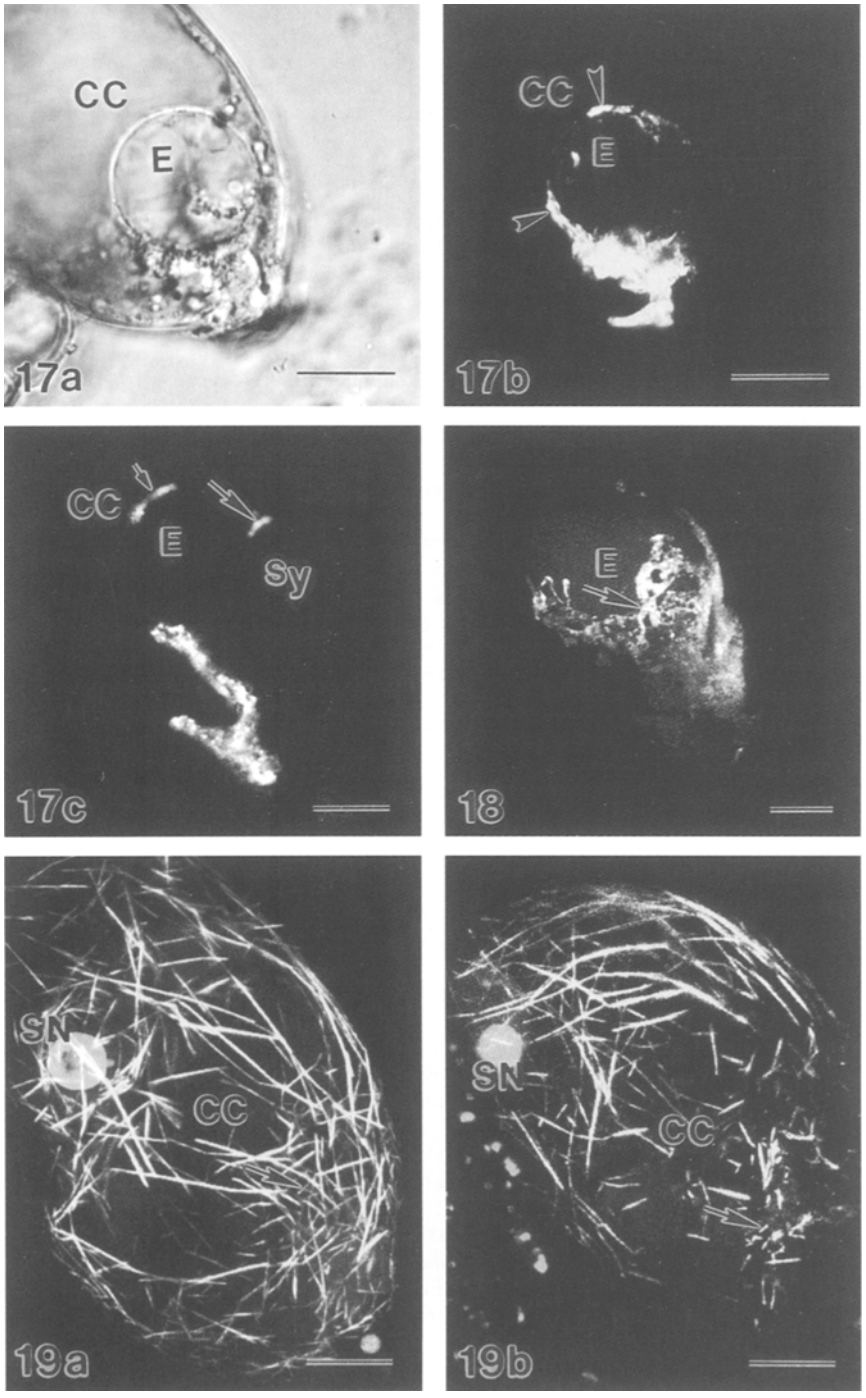

Fig. 17a–c. Labeling of actin in the intercellular space between the cells of the female germ unit at about 5 h after pollination but before the arrival of the pollen tube. **a** A transmissional image showing an egg cell (*E*) and a central cell (*CC*) (the synergids are not in focus) after pollination. Bar: 20 μm. **b** Labeling of actin with Alexa-phalloidin injection into the intercellular space between egg (*E*) and central cell (*CC*) in the same embryo sac as in **a**, showing a distinct actin corona (arrowheads) surrounding the egg cell. Bar: 20 μm. **c** Labeling of intercellular actin in another embryo sac with Alexa-phalloidin injection after pollination. Note that actin aggregates are localized between the egg (*E*) and the central cell (*CC*) (small arrow) and between the synergid (*Sy*) and the egg (large arrow). Bar: 10 μm

Fig. 18. Labeling of actin in the egg cell at 5 h after pollination, but before pollen tube arrival. Microinjection with Alexa-phalloidin into the egg cell (*E*) reveals the existence of actin patches (arrow) in the cell cortex after pollination. Bar: 10 μm

Fig. 19a, b. Actin organization in the central cell of *T. fournieri* before and after pollination. **a** Microinjection of Alexa-phalloidin into the central cell (*CC*) revealing an actin network in the cortical region. Note that the actin filaments are particularly dense in the perinuclear region of the secondary nucleus (*SN*) and the micropylar end of the central cell (arrow). **b** At 5 h after pollination, actin filaments become fragmented (arrow) in the micropylar end of the central cell (*CC*). *SN* Secondary nucleus. Bars: 10 μm

may be triggered by the arrival of the pollen tube, which correlates spatially and temporally with sperm penetration.

During fertilization dynamic changes of the actin cytoskeleton in the central cell appear to coincide with the migration of the secondary nucleus for the fusion with the male gamete. Before pollination two distinct arrays have been observed in the central cell, including a transversely oriented array in the cortex of the cell and an actin network in the cytoplasm. A similar network of actin filaments in the central cell has also been found in *Plumbago zeylanica* (Huang et al. 1993) and *Arabidopsis thaliana* (Webb and Gunning 1994). After pollination some actin bundles are found to

connect the secondary nucleus to the micropylar cortex of the central cell. The actin network in the micropylar end becomes fragmented. When the nuclear fusion takes place between a male gamete and central cell, the actin filaments become completely depolymerized into punctate structures at the perinuclear region (unpubl. obs.). Soon they reorganize as long filaments after fertilization, and the nucleus of the primary endosperm migrates back to the chalazal part of the cell and the endosperm rapidly reorganizes its cytoplasm (Mòl et al. 1994). Although the role of the actin arrays in the central cell is not fully understood, bundles of actin filaments appear to facilitate cytoplasmic streaming (Huang et al. 1992). Moreover, actin filaments have been postulated to be responsible for organelle transport and nuclear migration (Grolig 1998). Hence, they may play a similar role in the central cell during fertilization.

Acknowledgments

We thank Aline Valster, Jan Vos, and Luis Vidali for technical assistance in microinjection, and Dr. Terena Holdaway-Clarke for technical assistance operating the fluorescence microscope and image analysis software. We also acknowledge Ronald Bekwith for growing the plant material and Dale Callaham for help in operating the confocal microscope. We thank Prof. Edward Yeung for critical reading of the manuscript and Dr. Ming Yuan for providing two photographs in the present paper. The central Microscopy Facility of the University of Massachusetts is supported by a grant from the National Science Foundation (BBS 8714235). This research is supported by the RGC grant from the Research Grants Council of Hong Kong and the CRCG grant from University of Hong Kong to B.Q.H., the CRCG grant to S.Y.Z., and NSF grant no. MCB 9601087 to P.K.H.

References

Bednara J, Willemse MTM, van Lammeren AAM (1990) Organization of the actin cytoskeleton during megasporogenesis in *Gasteria verrucosa* visualized with fluorescent-labeled phalloidin. Acta Bot Neerl 39: 43–48

Chaubal R, Reger BJ (1990) Relatively high calcium is localized in synergid cells of wheat ovaries. Sex Plant Reprod 3: 98–102

– – (1992) The dynamics of calcium distribution in the synergid cells of wheat after pollination. Sex Plant Reprod 5: 206–213

Cleary AL (1995) F-actin redistribution at the division site in living *Tradescantia* stomatal complexes as revealed by microinjection of rhodamine-phalloidin. Protoplasma 185: 152–165

Doris FP, Steer MW (1996) Effects of fixatives and permeabilization buffer on pollen tubes: implications for localization of actin microfilaments using phalloidin staining. Protoplasma 195: 25–36

Grolig F (1998) Nuclear centering in *Spirogyra*: force integration by microfilaments along microtubules. Planta 204: 54–63

Hart NH, Fluck RA (1995) Cytoskeleton in *Toleost* eggs and early embryo: contribution to cytoarchitecture and mobile events. Curr Top Dev Biol 31: 343–381

Heslop-Harrison J, Heslop-Harrison Y (1991) The actin cytoskeleton in unfixed pollen tubes following microwave-accelerated DMSO-permeabilization and TRITC-phalloidin staining. Sex Plant Reprod 4: 6–11

Higashiyama T, Kuroiwa H, Kawano S, Kuroiwa T (1997) Kinetics of double fertilization in *Torenia fournieri* based on direct observations of the naked embryo sac. Planta 203: 101–110

Huang BQ, Russell SD (1992) Synergid degeneration in *Nicotiana*: a quantitative, fluorochromatic and chlorotetracycline study. Sex Plant Reprod 5: 151–155

– – (1994) Fertilization in *Nicotiana tabacum*: cytoskeletal modifications in the embryo sac during synergid degeneration. Planta 194: 200–214

– Sheridan FW (1994) Female gametophyte development in maize: microtubular organization and embryo sac polarity. Plant Cell 6: 845–861

– – (1998) Actin coronas in normal and indeterminate gametophyte embryo sacs of maize. Sex Plant Reprod 11: 257–264

– Pierson ES, Russell SD, Tiezzi A, Cresti M (1992) Video microscopic observations of living, isolated embryo sacs of *Nicotiana* and their component cells. Sex Plant Reprod 5: 156–162

– – – – (1993) Cytoskeletal organization and modification during pollen tube arrival, gamete delivery and fertilization in *Plumbago zeylanica*. Zygote 1: 143–154

Jensen WA (1974) Reproduction in flowering plants. In: Rodard AW (ed) Dynamic aspects of plants ultrastructure. McGraw-Hill, New York, pp 481–503

Keijzer CJ (1992) The isolation of sperm cells, their microinjection into the egg apparatus and method for structural analysis of the injected cells. In: Cresti M, Tiezzi A (eds) Sexual plant reproduction. Springer, Berlin Heidelberg New York Tokyo, pp 161–171

– Reinders MC, Leferink-ten Klooster HB (1988) A microinjection method for artificial fertilization in *Torenia*. In: Cresti M, Gori P, Pacini E (eds) Sexual reproduction in higher plants. Springer, Berlin Heidelberg New York Tokyo, pp 119–124

Lloyd CW (1989) The plant cytoskeleton. Curr Opin Cell Biol 1: 30–35

Miller DD, Scordilis SP, Hepler PK (1995) Identification and localization of three classes of myosins in pollen tubes of *Lilium longiflorum* and *Nicotiana alata*. J Cell Sci 108: 2549–2653

Mòl R, Matthys-Rochon E, Dumas C (1994) The kinetics of cytological events during double fertilization in *Zea mays* L. Plant J 5: 197–206

Palevitz BA, Tiezzi A (1992) Organization, composition, and function of the generative cell and sperm cytoskeleton. Int Rev Cytol 140: 149–185

Pierson ES, Cresti M (1992) Cytoskeleton and cytoplasmic organization of pollen and pollen tubes. Int Rev Cytol 140: 73–125

Russell SD (1982) Fertilization in *Plumbago zeylanica*: entry and discharge of the pollen tube into the embryo sac. Can J Bot 60: 2219–2230

– (1992) Double fertilization. Int Rev Cytol 140: 357–388

– (1996) Attraction and transport of male gametes for fertilization. Sex Plant Reprod 9: 337–342

Shimizu T (1995) Role of the cytoskeleton in the generation of spatial patterns in *Tubifex* eggs. Curr Top Devel Biol 31: 197–235

Sonobe S, Shibaoka H (1989) Cortical fine actin filaments in higher plant cells visualized by rhodamine-phalloidin after pretreatment with *m*-maleimidobenzoic acid N-hydroxysuccinimide ester. Protoplasma 148: 80–86

Swope RE, Kropf D (1993) Pronuclear position and migration during fertilization in *Pelvetia*. Dev Biol 157: 269–276

Valster AH, Hepler PK (1997) Caffeine inhibition of cytokinesis: effect on the phragmoplast cytoskeleton in living *Tradescantia* stamen hair cells. Protoplasma 196: 155–166

Vos JW, Hepler PK (1998) Calmodulin is uniformly distributed during cell division in living stamen hair cells of *Tradescantia virginiana*. Protoplasma 201: 158–171

Webb M, Gunning BES (1994) Cell biology of embryo sac development in *Arabidopsis*. In: Williams EG, Clarke AE, Knox RB (eds) Genetic control of self-incompatibility and reproductive development in flowering plants. Kluwer, Dordrecht, pp 461–485

Ye XL, Zee SY, Yeung EC (1997) Suspensor development in the Nun orchid, *Phaius tankervilliae*. Int J Plant Sci 158: 704–712